Available online at www.sciencedirect.com
SCIENCE DIRECT®
Catalysis Communications 5 (2004) 569–574
CATALYSIS COMMUNICATIONS
www.elsevier.com/locate/catcom

Radial distribution function studies of Al_2O_3–La_2O_3 binary oxides prepared by sol–gel

A. Barrera [a,b], M. Viniegra [a,*], V.H. Lara [a], P. Bosch-Giral [c]

[a] *Departamento de Química, UAM-Iztapalapa, Apdo. Postal 55-534, México, D.F 09340, Mexico*
[b] *Instituto Mexicano del Petróleo, Eje Central Lázaro Cárdenas 152, C.P. 07730 México, D.F, Mexico*
[c] *Instituto de Investigaciones en Materiales UNAM, México D.F, Mexico*

Received 30 October 2003; revised 7 May 2004; accepted 9 July 2004
Available online 20 August 2004

Abstract

The structure of Al_2O_3–xLa_2O_3 (x = 0, 2, 6, 15, 25, 50 wt%) binary oxides prepared via the sol–gel preparation method was studied by means of radial distribution functions determined from X-ray diffraction patterns. At first neighbors, the binary oxides are characterized by Al–O bond distances typical of γ-Al_2O_3. At second neighbors the binary oxides show La–O and O–O bond distances of La_2O_3. However, at higher coordination shells, these materials present bond distances corresponding to the mixed oxides with a perovskite-type structure. These structural differences of the binary oxides could be related to their differences in activity observed in the NO reduction with H_2.

Keywords: Al_2O_3; La_2O_3; Al_2O_3–La_2O_3; Mixed oxides; Sol–gel; Structure; Radial distribution function; NO reduction by H_2

1. Introduction

The addition of La_2O_3 to γ-alumina supports prevents sintering and increases thermal stability of noble metal catalysts [1–4]. Moreover, La_2O_3 addition to Pd-only three way catalysts improves the activity for the reduction of NO [5]. La_2O_3 is usually added by impregnating alumina with lanthanum solutions to obtain the La_2O_3/Al_2O_3 systems [6,7]. In these materials the structure is assumed to depend on both, the calcination temperature and the content of La_2O_3. Bettman et al. [3] found that a two-dimensional layer of La^{3+} ions is formed on the alumina surface at low lanthana content while at higher concentration, lanthanum occurs in the form of crystalline La_2O_3. They also suggested the formation of a surface lanthanum aluminate ($LaAlO_3$) after calcination at 800 °C. Similar results have been obtained by Haack et al. [4] and Oudet et al. [8], who reported the coexistence of $LaAlO_3$ and La_2O_3 phases at high lanthanum content. The formation of a perovskite-like phase when lanthanum oxide is supported on γ-Al_2O_3 was also reported by Alvarez et al. [9] from molecular dynamics simulation. Even though the structure of the La_2O_3/Al_2O_3 system has been extensively studied, the structure of the Al_2O_3–La_2O_3 binary oxides prepared by sol–gel has not been widely studied, yet particularly since these materials are homogeneous and amorphous [10–12]. Some characteristics of Pd catalysts supported on Al_2O_3–La_2O_3 prepared by sol–gel such as their desorption, reducibility, structural and textural properties have been reported before and together with their catalytic properties in the NO reduction with H_2 [11–14].

In this work, we studied the structural properties of Al_2O_3–La_2O_3 binary oxide supports prepared via the sol–gel method with a wide range of lanthana

* Corresponding author. Tel.: +52 555 804 46 65; fax: +52 555 804 46 66.
E-mail address: mvr@xanum.uam.mx (M. Viniegra).

1566-7367/$ - see front matter © 2004 Elsevier B.V. All rights reserved.
doi:10.1016/j.catcom.2004.07.007

concentration by means of their radial distribution function (RDF). In contrast to the oxides obtained by other preparation methods, the sol–gel materials are homogeneous and are characterized by an amorphous structure. The conventional diffraction patterns, therefore, cannot show structural details since a long-range order is not present. However, the determination of the RDF from the X-ray diffraction patterns can give information on the structural environment and the most probable interatomic distances in the vicinity of each atom. In this paper, we tried also to correlate the structure of Al_2O_3–La_2O_3 binary oxides prepared by sol–gel to their catalytic activity in the NO reduction with H_2.

2. Experimental

2.1. Preparation of Al_2O_3–La_2O_3 binary oxides

Al_2O_3–xLa_2O_3 binary oxides (Al–xLa, x = 0, 2, 6, 15, 25, 50 wt% La_2O_3) were prepared by the sol–gel method according to Masuda et al. [15], but with some modifications in the original procedure [11–14,16]. Briefly, Aluminum *sec*-butoxide Al(O-*Sec*But.)$_3$ (Alfa Aesar) and lanthanum acetylacetonate La(acac)$_3 \cdot x$H$_2$O (Alfa Aesar) were used as precursors of the La_2O_3–Al_2O_3 binary oxides. Samples were prepared by dissolving aluminum *sec*-butoxide in a solution containing ethanol (Aldrich) with a molar ratio ethanol/alkoxide = 1.1 and hexylene glycol (2-methylpentane-2,4-diol) (JT Baker) as a complexing agent with a molar ratio hexylenglicol/alkoxide = 0.86. Lanthanum acetylacetonate powder previously dissolved in ethanol (molar ratio ethanol/lanthanum acetylacetonate = 70) was added to the solution. The solution was heated with continuous stirring at 100 °C for 3 h. After cooling to room temperature, water with a H_2O/alkoxide molar ratio of 5.5 was added to the solution to perform the hydrolysis. The gels obtained were aged at 110 °C for 10 h and dried under vacuum at 110 °C. Then, they were treated under nitrogen flow (70 cm^3 min^{-1}) at 250 °C for 4 h and at 450 °C for 12 h, followed by calcination in an oven at 650 °C for 4 h. Pure alumina was prepared by the same method as the supports without addition of the lanthana precursor. Pure lanthana was prepared by dissolving lanthanum acetylacetonate powder in 1-butanol (Aldrich) with an 1-butanol/lanthanum acetylacetonate molar ratio of 19.4. The gel obtained was dried at 110 °C overnight, treated under N_2 flow at 450 °C for 12 h followed by calcination in an oven at 700 °C for 8 h.

2.2. Characterization

2.2.1. Surface area measurements

The specific surface area of Al_2O_3–La_2O_3 and pure La_2O_3, after calcination at 450 °C for 12 h in N_2, followed by a second calcination at 650 °C for 4 h for the binary oxides and at 700 °C for 8 h for pure lanthana, was obtained by nitrogen physisorption at −195 °C with an Autosorb gas sorption system from Quantachrome on the basis of the BET equation.

2.2.2. X-ray diffraction measurements

Conventional X-ray diffractograms were obtained with a Siemens D500 diffractometer coupled to a copper X-ray diffraction (XRD) tube. A diffracted beam monochromator releved the Cu Kα radiation. For radial distribution functions, X-ray diffraction patterns of Al_2O_3 and Al_2O_3–La_2O_3 samples calcined at 650 °C, for 4 h and La_2O_3 calcined at 700 °C for 8 h were obtained with the same Siemens D500 diffractometer coupled to a molybdenum anode X-ray tube to reach the required high values of the angular parameter $s = 4\pi \sin\theta/\lambda$, where θ is the diffraction angle and λ is the X-ray wavelength. The intensities and the angles measured by step scanning $\Delta 2\theta = (1/8)°$, from 2 to 120 °C, were the input data for the program Radiale [17]. The radial distribution functions were radial electron distributions, up to a radius of 10 Å. The resolution for small values of the radius was 0.01 Å.

2.3. Catalytic measurement

Reduction of NO with hydrogen over Al_2O_3–La_2O_3 samples calcined at 650 °C for 4 h and La_2O_3 calcined at 700 °C for 8 h was studied in a continuous flow micro-reactor Multipulse RIG 100 (In Situ Research Instrument) under atmospheric pressure in the 200–700 °C temperature range. Before the reaction the binary oxides (100 mg) were heated in flowing hydrogen (60 cm^3 min^{-1}) at 400 °C for 1 h. The reaction mixture in He was 5 vol% with a NO/H_2 molar ratio equal to 0.5 and a flow rate of 120 cm^3 min^{-1} (measured at room temperature and under atmospheric pressure). Each experimental run was carried out twice and samples were kept for 20 min at each temperature before collecting data. Analysis of NO, N_2, N_2O, and NH_3 was performed in a gas chromatograph equipped with a thermal conductivity detector.

2.4. Results and discussion

Fig. 1 shows the BET surface area (S_{BET}) of the Al_2O_3–La_2O_3 binary oxides. The S_{BET} reaches a maximum value for the Al–La-15 binary oxide whichever the thermal treatment (415 m^2 g^{-1} at 450 °C and 284 m^2 g^{-1} at 650 °C). The S_{BET} is also high for Al–La-25, while it decreases to 120 m^2 g^{-1} for Al–La-50. The composition at which the maximum surface area is obtained (Al–La-15) is in disagreement with the results of Subramanian et al. [18] who suggested that 8 wt% La_2O_3 would be the optimum lanthana loading in order to

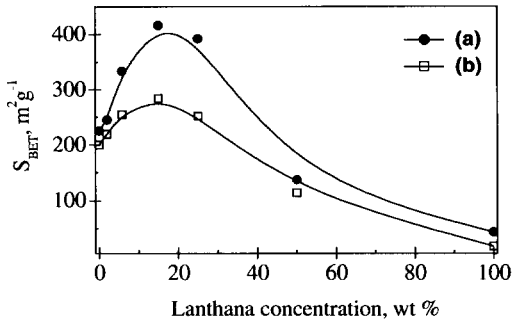

Fig. 1. BET surface area of Al_2O_3–La_2O_3 binary oxides as a function of La_2O_3 content: (a) after calcination at 450 °C for 12 h; (b) after the treatment given in (a) followed by calcination at 650 °C for 4 h for the binary oxides, and at 700 °C for 8 h for pure La_2O_3.

maximize the surface area when La_2O_3 is impregnated onto γ-Al_2O_3. The difference between the two preparation methods could be that in impregnated alumina most of La_2O_3 is located on the surface of the alumina whereas by sol–gel, La_2O_3 is highly dispersed within the structure of alumina. This is corroborated by the X-ray diffraction patterns (Fig. 2(a)). For low La_2O_3 content, the only phase detected is that of γ-Al_2O_3. At higher lanthana concentration the intensity of the reflexion peaks associated to γ-Al_2O_3 decreases and the diffraction patterns appear to be almost flat, similar to those of a non structured material. It seems that increasing the concentration of lanthana introduces disorder into the initial γ-Al_2O_3 spinel structure. However, a broad peak in the range of $2\theta = 25$–$35°$ with a very low intensity is observed in the XRD patterns of Al–La-25 and Al–La-50 binary oxides suggesting the presence of La_2O_3. This feature can be assigned to crystalline La_2O_3 since the diffraction pattern of this oxide presents the most intense peak at $2\theta = 30°$ (Fig. 3).

Fig. 4 compares the radial distribution functions of the monometallic oxides, and Table 1 summarizes the position of the peaks and the associated phase. The assignations have been made on the basis of effective ionic radii calculations and the results reported by Capitán [19] and Alvarez [9] obtained by molecular dynamic calculations. The radial distribution functions obtained theoretically correspond to bond distances by paires. In X-ray diffraction the radial distribution functions is determined by all bond distances. In the first coordination sphere alumina (Fig. 4(a)) presents a clear and intense peak at 1.9 Å that corresponds to the Al–O bond length. This bond distance value is in good agreement with the radial electron distribution calculations of Léonard et al. [20,21], who reported the average Al–O bond length in γ-Al_2O_3 in the range 1.82–1.88 Å. In the lanthanum oxide curve (Fig. 4(b)), the first coordination sphere is situated at 2.45 Å, it may be assigned to the La–O bond distance according to the ionic radii calculation.

The RDF curve of alumina also shows a peak at a radius of 3.14 Å which can be attributed to the Al–Al bond distance [19]. The alumina RDF curve shows also a peak situated at a radius of 4.55 Å. This peak results from the overlap of the RDF peaks at a radius of 4.38

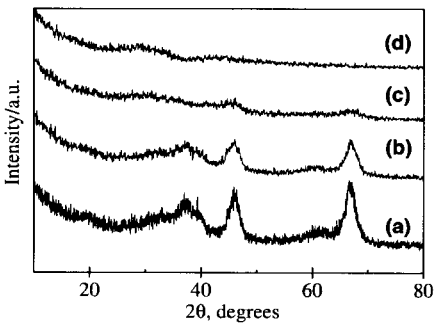

Fig. 2. Conventional X-ray diffraction patterns of Al_2O_3–La_2O_3 binary oxides calcined at 650 °C for 4 h: (a) Al_2O_3; (b) Al–La-15; (c) Al–La-25; (d) Al–La-50.

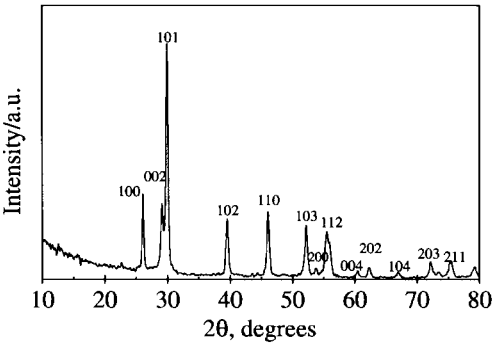

Fig. 3. Conventional X-ray diffraction pattern of La_2O_3 calcined at 700 °C for 8 h.

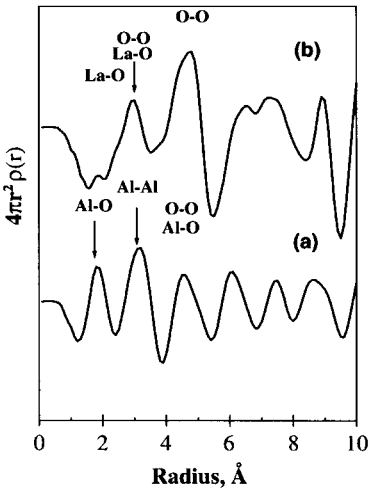

Fig. 4. Radial distribution function of simple oxides: (a) Al_2O_3 calcined at 650 °C for 4 h; (b) La_2O_3 calcined at 700 °C for 8 h.

Table 1
Position of the radial distribution function peaks of Al_2O_3 and La_2O_3

Al_2O_3 r (Å) (this work)	Al_2O_3 (cubic spinel) r (Å) [13]			La_2O_3 r (Å) (this work)	La_2O_3 r (Å)	
	Al–O	O–O	Al–Al		La–O	O–O
1.90	1.87					
				2.45	2.48[a]	
				2.90	2.88[a]	2.80[a]
3.14			3.03			
4.55	4.38	4.84		4.81		4.83[b]
6.07						
				6.58		6.62[b]
				7.35		
7.46						
8.66						
				8.91		

[a] Ionic radii calculation.
[b] Ref. [13].

and 4.84 Å. These peaks correspond to the Al–O and O–O bond distances, respectively, for the cubic spinel structure according to molecular dynamics simulation [19]. La_2O_3 presents a peak at 2.9 Å which is attributed to both the La–O and O–O bonds considering the hexagonal structure of La_2O_3 and according to the ionic radii calculation. Other peaks appear at 4.81 and 6.58 Å in the RDF of La_2O_3 which are attributed to O–O bonds of the cubic system according to molecular dynamics simulation [19].

On the other hand, the radial distribution functions of the Al_2O_3–La_2O_3 binary oxides for lanthana concentration $\geqslant$ 15 wt% are compared in Fig. 5, and the corresponding position of the peaks are shown in Table 2. All the binary oxides show a first peak at a radius of 1.9 Å that decreases in intensity with lanthana concentration. This peak is assigned to the Al–O bond observed in γ-Al_2O_3 (Fig. 4). The second peak has a shoulder at 2.9 Å which is attributed to the presence

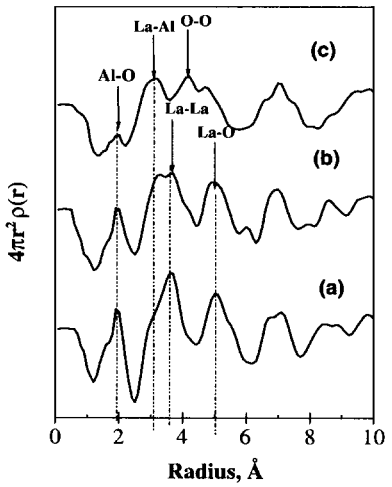

Fig. 5. Radial distribution function of Al_2O_3–La_2O_3 binary oxides calcined at 650 °C for 4 h: (a) Al–La-15; (b) Al–La-25, (c) Al–La-50.

of both La–O and O–O bonds of La_2O_3 according to its radial distribution function (Fig. 4).

In all the RDF curves of binary oxides some peaks appear that are not present in La_2O_3 or in γ-Al_2O_3 radial distibution functions. This suggests that there are several types of bonds in the binary oxides that do not occur in the simple oxides. Besides, the number of this type of bonds increases for La_2O_3 concentrations higher than 15 wt%. The RDF curve of Al–La-15 binary oxide shows a sharp peak at a radius of 3.64 Å. This peak does not appear in the FDR of La_2O_3 or γ-Al_2O_3 and is attributed to the presence of La–La bond distances of La_2O_3 with cubic structure [19]. This observation suggests the coexistence of La_2O_3 phases both in the hexagonal and cubic system in the binary oxides. This peak is also present in the RDF of Al–La-25 binary oxide, and we can also observe the appearance of another one at a radius of 3.19 Å. This peak is assigned to the presence of mixed oxides La–Al bond distances with an ideal perovskite-type structure ($LaAlO_3$) [9], and is more clearly observed in the RDF of Al–La-50 binary oxide. For this binary oxide the peak at 3.64 Å, attributed to cubic La_2O_3, disappears and two new peaks appear at 4.18 and 4.77 Å which are assigned to O–O and La–O bonds found in the mixed oxide with a perovskite-type structure [19]. The perovskite type structure is the origin of the peaks at 5.0, 6.02, 6.76 and 6.86 Å, while the peak at 6.61 Å is attributed to the O–O distance within the cubic structure of La_2O_3 [9,19]. Therefore, besides the presence of crystalline La_2O_3, some micro domains corresponding to the mixed oxide phases with a perovskite-type structure are present in the Al_2O_3–La_2O_3 binary oxides prepared by sol–gel. When the Al–La-50 binary oxide is calcined at 1000 °C there is a phase transformation from the amorphous to the crystalline state and its identification corresponds to $LaAlO_3$ with a perovskite structure [16]. This phase was also identified in the Al_2O_3–La_2O_3 binary oxide prepared by sol–gel with 5.8 wt% La_2O_3 after calcination at 1200 °C [11].

Table 2
Position of the radial distribution function peaks of Al_2O_3–La_2O_3 binary oxides

Al_2O_3 r (Å)	La_2O_3 r (Å)			Al–La-15 r (Å) (this work)	Al–La-25 r (Å) (this work)	Al–La-50 r (Å) (this work)	Perovskite-type structure (Å)			
Al–O	La–O	O–O	La–La				La–Al	La–O	O–O	O–La
1.90				1.90	1.90	1.90				
	2.90	2.90		2.90	2.90	2.90				
					3.19	3.19	3.21[a]			
			3.68[b]	3.64	3.64					
						4.18			4.17[b]	
						4.77		4.73	4.83[b]	
				5.10	5.10			5.00[a]		
					6.02					6.00[b]
		6.62				6.61				
				6.76					6.77[a]	
					6.86					6.90[b]

[a] Ref. [9].
[b] Ref. [13].

Catalytic activity ($NO/H_2 = 0.5$) results of the binary oxides in terms of the NO conversion % divided by the surface area are shown in Fig. 6. Pure γ-Al_2O_3 is active only at temperatures higher than 500 °C, while the binary oxides are active at 250 °C with Al–La-50 being the more active. However, La_2O_3 is considerably the most active material at temperatures higher than 400 °C (Fig. 6). The radial distribution function studies showed that the structure of Al–La-50 binary oxide is different, at the short range order, and the RDF peaks corresponding to bond distances of the provskite-type structure are more clearly defined. Besides, in the RDF of Al–La-50 a peak at 6.62 Å appears that is assigned to O–O bonds of cubic La_2O_3. The presence of bonds corresponding to the perovskite-type structure could be also related to the formation of some micro domains of the lanthanum hexaluminate phase ($LaAl_{11}O_{18}$) which was detected by HRTEM in the Al–La-50 sample [16]. On the other hand, some authors [22–26] have suggested that the NO decomposition on La_2O_3 and the selective reduction of NO on La_2O_3/Al_2O_3 takes place by the NO adsorption onto oxygen vacancies sites localized in the La_2O_3 structural lattice. According to Vannice et al. [24,25], the formation of these vacancies

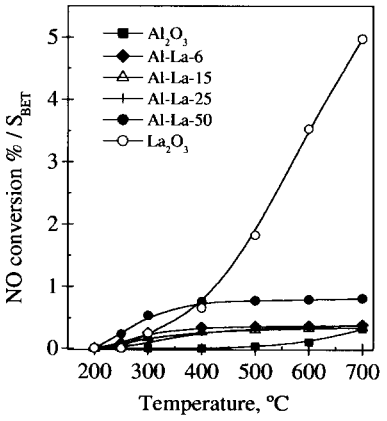

Fig. 6. NO conversion %/S_{BET} vs. reaction temperature ($NO/H_2 = 0.5$) over Al_2O_3–La_2O_3 binary oxides calcined at 650 °C for 4 h and over La_2O_3 calcined at 700 °C for 8 h.

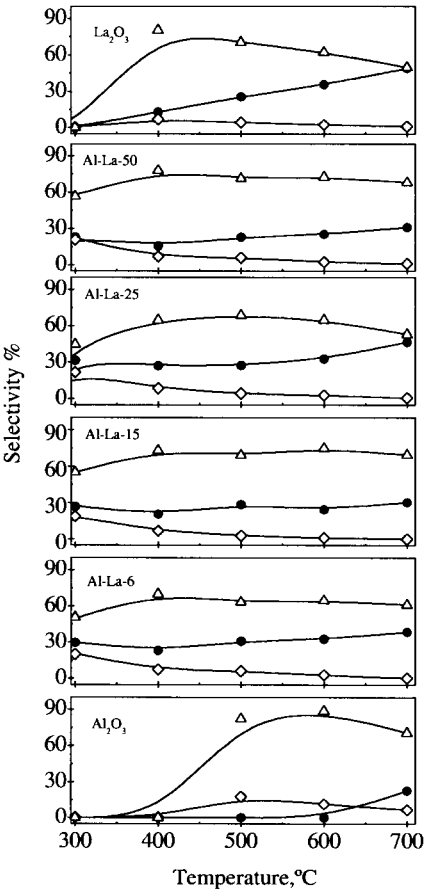

Fig. 7. Selectivity % vs. reaction temperature ($NO/H_2 = 0.5$) over Al_2O_3–La_2O_3 binary oxides calcined at 650 °C for 4 h and over La_2O_3 calcined at 700 °C for 8 h: ● = N_2, ◇ = N_2O, △ = NH_3.

may occur during the pretreatment of the oxides, while their density in La_2O_3/Al_2O_3 depends on lanthana concentration. Thereby, according to this model the concentration of oxygen vacancies in the Al_2O_3–La_2O_3 system should increase with La_2O_3 concentration and this could be the reason for which Al–La-50 and La_2O_3 are the most active materials when the surface area is considered. Therefore, according to the model of Winter [26] the anion vacancies present in the La_2O_3 phases could be responsible for the NO dissociation and the catalytic behavior observed in the binary oxides.

On the other hand, Fig. 7 shows the selectivity of the oxides for the NO + H_2 reaction. NH_3 is the main product and formation of N_2O is low and decreases as the reaction temperature is increased for all the samples. γ-Al_2O_3 does not produce N_2 at temperatures lower than 600 °C, and when La_2O_3 is added, selectivity to N_2 increases to ca. 10–45% for all the temperature range studied. It seems that the modification of alumina by adding lanthana influences directly the N_2 formation due to a higher capability of the mixed oxides for the dissociation of NO.

2.5. Conclusions

The structure of the Al_2O_3–La_2O_3 binary oxide supports prepared by sol–gel was determined by radial distribution functions. At first neighbors, the binary oxides are characterized by Al–O bond distances typical of γ-Al_2O_3. At second neighbors the binary oxides show La–O and O–O bond distances corresponding to the La_2O_3 phase. However, at higher coordination shells, these materials present bond distances corresponding to the mixed oxides with a perovskite-type structure. The number of these bonds increases with lanthana concentration. The presence of La–Al bonds can be detected for La_2O_3 contents higher than 15 wt%. The binary oxide with 50 wt% of La_2O_3 also shows bond distances corresponding to the cubic La_2O_3. These structural differences of the binary oxides could be related to the differences in activity observed in the NO reduction with H_2.

Acknowledgements

The authors thank to M.C.A. Gómez-Cortés (IFUNAM) for his technical assistance in the activity measurements. A. Barrera thanks to CONACYT for the scholarship granted.

References

[1] H. Schaper, E.B.M. Doesburg, L.L. van Reijen, Appl. Catal. 7 (1983) 211.
[2] H. Schaper, D.J. Amez, E.B.M. Doesburg, L.L. van Reijen, Appl. Catal. 9 (1984) 124.
[3] M. Bettmann, R.E. Chase, K. Otto, W.H. Weber, J. Catal. 117 (1989) 447.
[4] L.P. Haack, J.E. de Vries, K. Otto, M.S. Chattha, Appl. Catal. 117 (1989) 477.
[5] H. Muraki, K. Yokota, Y. Fujitani, Appl. Catal. 48 (1989) 93.
[6] M.J. Capitán, M.A. Centeno, P. Malet, I. Carrizosa, J.A. Odriozola, A. Márquez, J.F. Sanz, J. Phys. Chem. 99 (1995) 4655.
[7] M. Scheithauer, H. Knôzinger, M.A. Vannice, J. Catal. 178 (1998) 701.
[8] F. Oudet, P. Courtine, A. Vejux, J. Catal. 114 (1988) 112.
[9] L.J. Alvarez, J.F. Sanz, M.J. Capitán, J.A. Odriozola, Catal. Lett. 21 (1993) 89.
[10] K. Tadanaga, H. Kobayashi, T. Minami, J. Non-Cryst. Solids 225 (1998) 230.
[11] N.E. Bogdanchikova, S. Fuentes, M. Avalos-Borja, M.H. Farías, A. Boronin, G. Díaz, Appl. Catal. B 17 (1998) 221.
[12] S. Fuentes, N. Bogdanchikova, M. Avalos-Borja, A. Boronin, M.H. Farías, G. Díaz, A.G. Cortes, A. Barrera, Catal. Today 55 (2000) 301.
[13] S. Fuentes, N.E. Bogdanchikova, G. Diaz, M. Peraaza, G.C. Sandoval, Catal. Lett. 47 (1997) 27.
[14] A. Barrera, M. Viniegra, P. Bosch, V.H. Lara, S. Fuentes, Appl. Catal. B 34 (2) (2001) 97.
[15] K. Masuda, M. Kawai, K. Kuno, N. Kachi, F. Mizukami, in: Preparation of Catalysts, in: V.G. Poncelet, P.A. Jacobs, P. Grange (Eds.), Studies of Surface Science Catalysis, vol. 63, Elsevier, Amsterdam, 1991, p. 229.
[16] A. Barrera, Ph.D. Thesis, Universidad Autónoma Metropolitana – Iztapalapa, México D.F, 2003.
[17] M. Magini, A. Cabrini, J. Appl. Cryst. 5 (1972) 14.
[18] S. Subramanian, M.S. Chattha, C.R. Peteres, J. Mol. Catal. 69 (1991) 235.
[19] M.J. Capitán, Ph.D. Thesis, Universidad de Sevilla, Sevilla Spain, 1993.
[20] A.J. Léonard, P.N. Semaille, J.J. Fripat, Proc. Br. Ceram. Soc. 103 (1969).
[21] H. Knozinger, P. Ratnasamy, Catal. Rev. Sci. Eng. 17 (1) (1978) 31–70.
[22] B. Klingenberg, M.A. Vannice, Appl. Catal. B 21 (1999) 19.
[23] S.J. Huang, A.B. Walters, M.A. Vannice, J. Catal. 192 (2000) 29.
[24] S.J. Huang, A.B. Walters, M.A. Vannice, Appl. Catal. B 26 (2000) 101.
[25] M. Scheitahuer, H. Knözinger, M.A. Vannice, J. Catal. 178 (1998) 791.
[26] E.R.S. Winter, J. Chem. Soc. A (1968) 2889.